JOURNAL OF MATERIALS SCIENCE **38** (2003) 1565–1572

Indentation responses of plasma sprayed ceramic coatings

S. GHOSH*, S. DAS‡, T. K. BANDYOPADHYAY‡, P. P. BANDYOPADHYAY*,§, A. B. CHATTOPADHYAY*
*Departments of *Mechanical Engineering and ‡Metallurgical and Materials Engineering, Indian Institute of Technology, Kharagpur 721 302, India*
E-mail: sdas@metal.iitkgp.ernet.in

This investigation aims at finding the Vickers and Knoop indentation responses of a few plasma sprayed ceramic coatings, namely Indian alumina, imported alumina, zircon, plasma dissociated zircon (PDZ) and zircon—20 wt% CaO. Some of the sprayed coatings under Vickers indentation show typical Indentation Size Effect (ISE) while others exhibit Reverse Indentation Size Effect (RISE). Such coating behaviour may be attributed to the heterogeneous phase composition and microstructure of the coatings. "True Hardness" and "Elastic Modulus" of the ceramic coatings have been calculated. Also the ISE phenomenon observed for all the coatings undergoing Knoop indentation are explained using models such as Meyer's law, Normalised Meyer's law, Hays' Kendall Approach and Proportional Resistance models. These models have so far been used for explaining the ISE behaviour of only the sintered crystalline ceramics. In this paper, it has been shown that these models hold good to an appreciable extent for plasma sprayed ceramic coatings as well.

1. Introduction

The microhardness indentation technique using a Vickers diamond pyramidal indenter is a simple method for studying the elastic-plastic response of materials. Symmetrical and regular cracking is often produced in dense ceramics because of Vickers indentation and the imprint is used to obtain estimates of the fracture toughness (K_{IC}) value. The method of indentation thus provides a quick and easy means to estimate the K_{IC} values of materials using small specimens [1].

In this investigation, the hardness and cracking behaviour of some plasma sprayed ceramic coatings on steel substrates have been studied using Vickers and Knoop indentation. The variation of microhardness with increasing test load for various plasma sprayed coatings has been noted and a plausible explanation for this type of behaviour has been put forward. The true hardness of the coatings has been determined using the approach followed by Li *et al.* [2].

The elastic modulus, E, of the coatings has been calculated based on the dimensions of the Knoop indentation. The E value of the plasma sprayed ceramic coatings is known to be much lower than that of the bulk materials. This is owing to the unique microstructure, and inhomogenities associated with such thermal spray deposition. There are several ways of determining the E values of plasma sprayed coatings such as bending, ring and tensile tests. One widely used method of obtaining E value of thermal spray deposits is by performing stress-strain tests on freestanding ceramics. However, obtaining a sufficiently large freestanding thermally sprayed ceramic sample is quite difficult. Methods other than indentation are rather complex and inappropriate to acquire engineering data routinely [3, 4]. A simple technique to assess the hardness-elastic modulus ratio (H/E) based on the measurement of the elastic recovery of the in-surface dimensions of Knoop indentation imprint has been used by Marshall *et al.* [5]. In this technique, the H/E value has been derived from the measured values of the major and the minor diagonals of a Knoop indentation. In the full loaded state, the ratio of the minor to the major diagonal of a Knoop indentation should be 0.14 as determined by the Knoop indenter geometry. However, owing to the elastic recovery, the fractional change in length of the minor diagonal is much more than that of the major diagonal. This elastic recovery is related to the H/E ratio. The advantage of this type of test lies in the fact that the hardness and the elastic modulus of the specimen can be obtained simultaneously.

It has been observed that hardness for most materials is a function of the test load. Calculation of fracture toughness by the indentation method requires the use of hardness value. The calculated K_{IC} values can vary significantly depending on the hardness values used [6, 7]. Thus, determination of a load independent true hardness of materials is important [1].

§*Present Address*: B. E. College, Howrah 711 103, India.

For the Knoop indentation measurements, the true hardness is defined as

$$H_o = 14229\, P/d_o^2 \text{ (GPa)} \quad (1)$$

where P is the applied load and d_o is the sum of as-measured Knoop indentation diagonal (d), and the relaxation correction, (d_e), i.e., $d_o = d + d_e$.

The d_e part may be taken as a correction factor, which is related to elastic relaxation and indentation size effects, such as the surface tension, the crack formation, and the dislocation activity [8].

It is known that the knoop hardness can be expressed by the following equation:

$$H_k = 14229\, P/d^2 \text{ (GPa)} \quad (2)$$

Combining Equations 1 and 2 we get,

$$H_k = H_o\{1 + d_e/d\}^2 \quad (3)$$

Since d may be the same magnitude as d_e at low loads, the hardness H_k becomes load dependent in the low load regime, but at higher loads the ratio of d_e/d is much less than unity and then the measured H_k reveals a test load independence and hence is referred to, as true hardness, H_o. However, the true hardness value can be calculated by another method. Substitution of the value of d_o by $(d + d_e)$ in Equation 1 gives the following equation:

$$d = (14229/H_o)^{1/2} P^{1/2} - d_e \quad (4)$$

Thus if a plot of the as-measured major diagonal, d, and $P^{1/2}$ is made, then the slope of the straight line gives the true hardness [2].

Knoop indentation measurements can also be used to evaluate the H/E ratio of the specimens based on measuring the elastic recovery of the indentation. This elastic recovery actually reduces the length of the minor diagonal of the indentations as well as the residual indentation depth, whereas the change in length of the major diagonal is negligible. The model that relates the displacement of the minor diagonal and H/E ratio is obtained using the superposition of solutions for an elliptical hole subjected to uniaxial stress [9].

$$b - b' = \alpha a p/E \quad (5a)$$

$$a - a' = \alpha b p/E \quad (5b)$$

where a = half major diagonal before elastic recovery, a' = half major diagonal after elastic recovery, b = half minor diagonal before elastic recovery, b' = half minor diagonal after elastic recovery, and $\alpha = 1.5$ as predicted by the elliptical model.

Since the elastic recovery along the major diagonal is insignificant [10], it can be assumed that $a' = a$, and replacing p with H Equation 5a becomes

$$b'/a' = b/a - \alpha H/E \quad (6)$$

The value of α has been experimentally found by Marshall *et al.* [5] to be 0.45, which is much lower than the theoretically predicted value of 1.5. This apparently is owing to the smaller elastic recovery in the constrained Knoop indentation zone. In this present study the α value is taken as 0.45.

2. Experimental procedure

Various types of ceramic powders, namely, Indian alumina, imported alumina, zircon sand, plasma dissociated zicon (PDZ) and zircon-20 wt% CaO have been plasma sprayed onto mild steel substrates of dimensions 125 mm × 13 mm × 5 mm using a plasma spraying equipment of capacity of 40 kW. Although the powders mentioned above, except for the imported alumina do not belong to the so called "plasma-sprayable" category of powders, these cheap commercially available powders could be plasma sprayed to form coatings of sound quality [11]. Before spraying, the mild steel substrates have been shot blasted with alumina grits (grit size 60). Immediately after shot blasting the substrates have been cleaned using trichloroethylene and isopropyl alcohol in an ultrasonic cleaner. The cleaned specimens are plasma sprayed with a Ni-5 wt% Al bond coat and subsequently various top coats have also been applied. Immediately after spraying, test coupons of dimensions 13 mm × 13 mm × 5 mm have been cut off from the larger samples. These specimens after an initial grinding on silicon carbide papers have been subjected to polishing using diamond pastes. The polished samples have been indented first with a Vickers indenter using loads of 25, 50, 100, 200, 300, and 500 grams consecutively and a dwell time of 20 seconds have been used. The same procedure has been repeated using a Knoop indenter. For both cases, diagonal lengths of the impression left by the indenter on the surface have been measured. At each load, a minimum of ten good indentations have been made and their diagonal lengths have been measured.

3. Results and discussions

3.1. Analysis of the Vicker's hardness data

The Indian alumina coating shows the typical Indentation Size Effect (ISE) as is evident from the plot of Vickers' hardness as a function of test loads (Fig. 1). With increasing test load, the apparent microhardness value of this coating decreases and this type of phenomenon can be explained by the Proportional Specimen Resistance Model (PSR) [12, 13]. An interesting thing to note is that, the hardness value of this alumina coating is much lower than that of sintered alumina. This can be attributed to the unique microstructure of the plasma sprayed ceramics.

Fig. 2 shows the hardness-load characteristics of alumina coating made of imported, plasma sprayable grade consumable. This alumina coating is somewhat softer than its indigenous counterpart presumably owing to the presence of a large number of hard metastable alumina phases in the Indian alumina coating (Table I). For this coating, surface cracks are observed at an indentation load of 200 gm, which suggests that the coating is quite dense. For this coating, it is observed that the

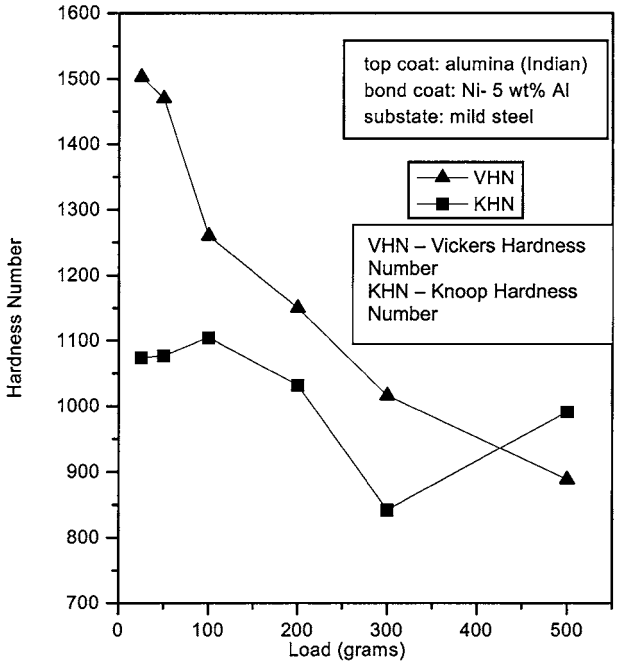

Figure 1 Variation of hardness with load for Indian alumina coating.

TABLE I The XRD data for various coatings

Sl. no	Material	Particulars of peaks	Remarks
1	Indian alumina coating	α-alumina-9 peaks β-alumina-1 peak ε-alumina-1 peak τ-alumina-1 peak κ'-alumina-3 peaks θ-alumina-2 peaks	
2	Imported alumina coating	α-alumina-5 peaks β-alumina-1 peak Kl-alumina-2 peaks	
3	PDZ coating (as coated)	Zircon-none m-z-4 peaks t-z-3 peaks c-z-6 peaks	t-z peaks are at (110), (102) and (103)
4	Zircon-20 wt% CaO (as sprayed)	Zircon-2 peaks m-z-2 peaks t-z-1 peaks c-z-7 peaks	

m-z: monoclinic zirconia, t-z: tetragonal zirconia, c-z: cubic zirconia.

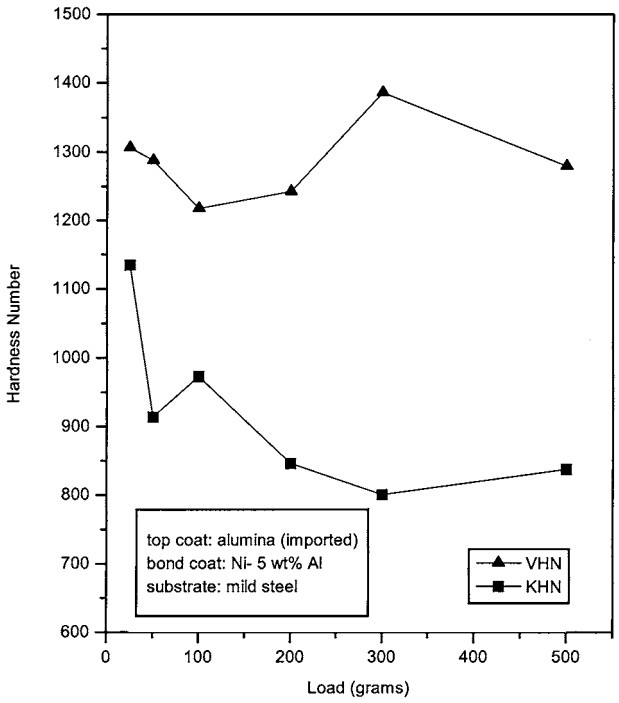

Figure 2 Variation of hardness with load for Imported alumina coating.

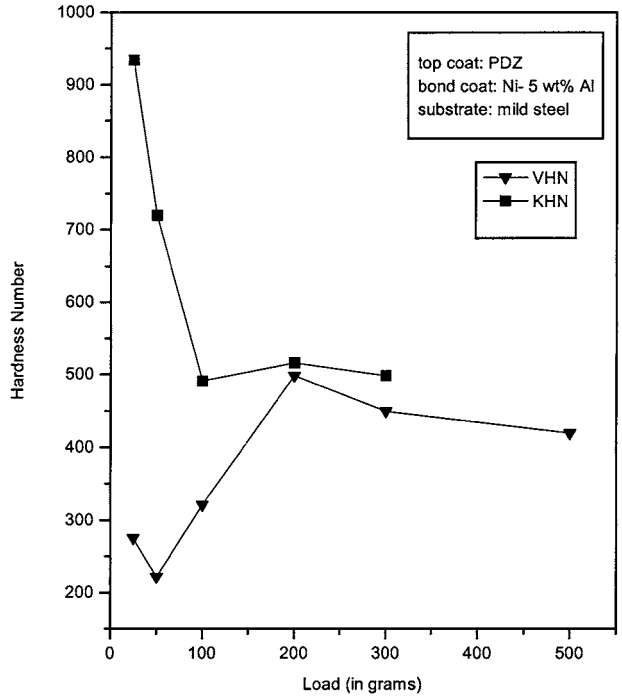

Figure 3 Variation of hardness with load for PDZ coating.

microhardness value first decreases with load and upon reaching a certain load the hardness starts to increase. Therefore, the coating is showing an Indentation Size Effect al low load but at the higher loads it is exhibiting a reversal of the Indentation Size Effect presumably owing to crack generation at higher loads. In such cases, a fraction of the energy imparted to the specimen is spent in crack propagation [14].

Fig. 3 shows the hardness-load characteristics of the Plasma Dissociated Zircon coating. The plasma dissociated zircon coating is much softer than both alumina coatings. It is interesting to note that here the hardness of this coating increases almost continuously with an increase in indentation load, and it is a reversal of the Indentation Size Effect. This phenomenon is termed as Reverse Indentation Size Effect (RISE) [14]. RISE has been studied for wrought and sintered materials. For metallic samples such behaviour is attributed to work hardening induced in the localized region around the indentation site during indentation. For brittle materials, it is a common observation that cracking occurs during the indenter loading half-cycle. Feltham and Banerjee [14] first suggested that the RISE might be related to the energy loss owing to the cracking of the specimens during the indentation. Owing to such cracking, a fraction of energy is spent in crack propagation and a small indentation size results. Hence, the indentation test yields an apparently high hardness value [15].

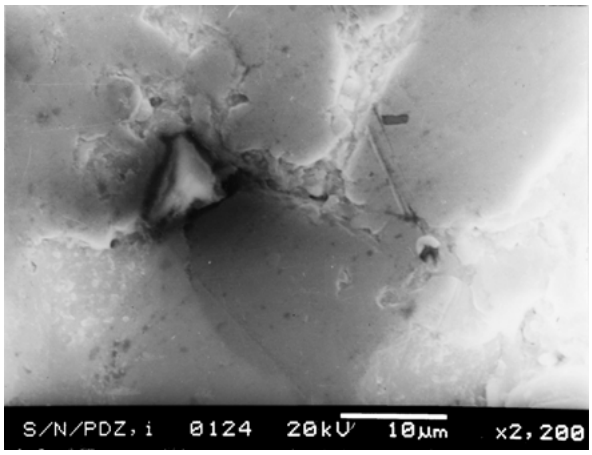

Figure 4 The polished top surface of the PDZ coating showing the occurrence of a crack in the vicinity of the indentation.

In the case of the PDZ coating microcracking is observed. A typical case is depicted in Fig. 4. This coating is a two-phase aggregate comprising of zirconia and silica phase. The XRD pattern of the as-sprayed PDZ coating (Table I) shows the presence of all the three polymorphs of zirconia, i.e., high temperature cubic phase, tetragonal phase and the room temperature monoclinic phase. The silica phase, however, remains in an amorphous state and hence no corresponding peak is observed in the XRD pattern. Owing to the presence of this glassy phase the gross hardness values of these coatings are low. During the loading half cycle, median cracks develop and they can be seen on the surface immediately after the unloading of the indenter. This cracking phenomenon increases the apparent microhardness because a part of the energy during indentation is consumed in cracking. In addition, it may so happen that during the indenter penetration, the stress field generated around the indenter tip is sufficiently high to bring about a martensitic transformation of the metastable tetragonal zirconia phase to the room temperature monoclinic zirconia phase. This transformation is associated with a 2–3% volume expansion and consequently, owing to this volume expansion, the final size of the impression left by the indenter on the coating surface may get reduced resulting in an apparently higher hardness value.

The Vicker's hardness response of zircon coating also shows a trend similar to the PDZ coating (Fig. 5). This is expected, since the zircon coating is similar to the PDZ coating with the exception that during plasma spraying the zircon gets dissociated into zirconia and silica, whereas in the case of the PDZ, the zirconia and silica remain separate at the point of injection of the powder into the plasma flame [16]. The low hardness value for this coating may also be attributed to the presence of the glassy silica phase in the coating. This specimen also shows cracking on the surface and exhibits the RISE phenomenon owing to the same reasons, as stated for the PDZ coating.

The hardness values for the zircon-20 wt% calcia coatings are found to be much higher than that of the PDZ or the zircon coatings (Fig. 6). This may be owing to the presence of a greater amount of the harder cubic

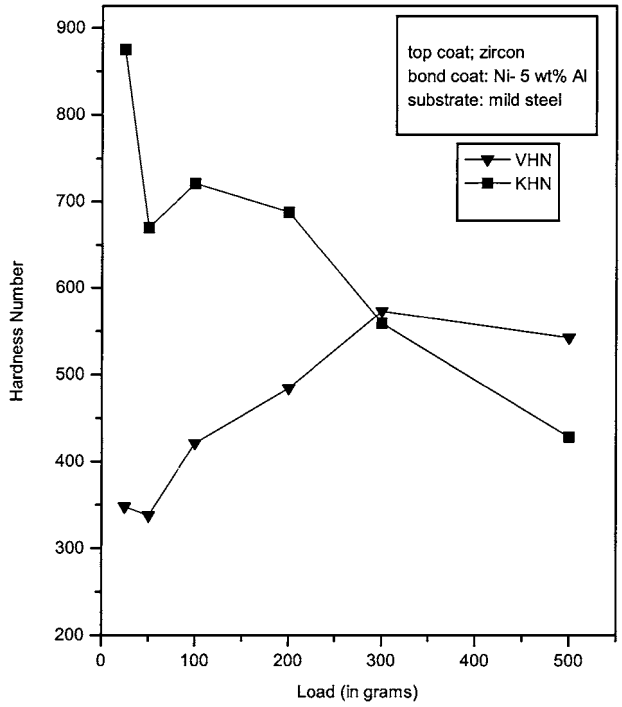

Figure 5 Variation of hardness with load for Zircon coating.

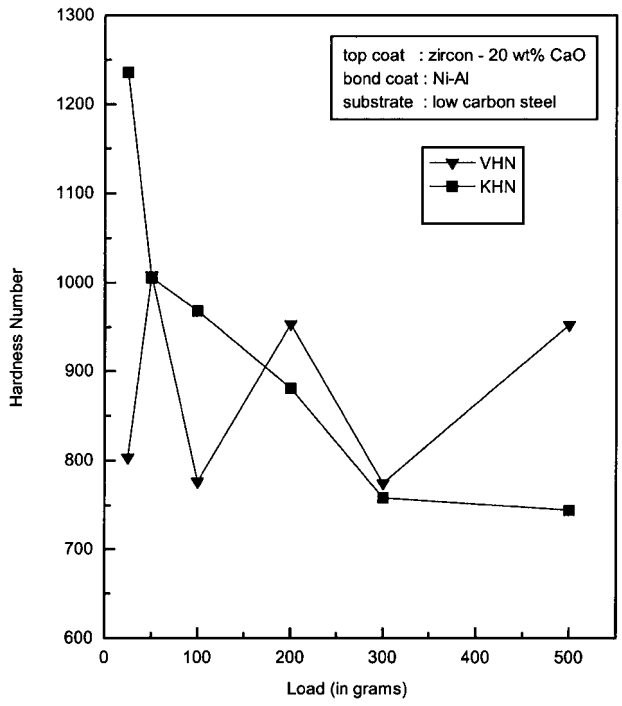

Figure 6 Variation of hardness with load for Zircon 20 wt% CaO coating.

zirconia phase as observed in the XRD data of the as-sprayed zircon-20 wt% CaO coating (Table I). Actually, an increase in the amount of the cubic zirconia phase is owing to a chemical stabilisation of this particular phase brought about by the addition of calcia. There is however no definite trend of the hardness values with increasing indentation loads.

3.2. Analysis of the Knoop hardness data

A linear curve fitting of $P^{1/2}$ and the Knoop indentation major diagonal (d) data for all samples shows that there

TABLE II True hardness values, correlation coefficients (r^2), Mayer's law coefficients (A and n), normalized Mayer's law coefficients (A_o and n'), the critical loads (P_c) and characteristics indentation diagonal (d_o) of the coatings under study

Sample type	r^2	True hardness, H_o (GPa)	A (g/μm^{-n})	n	P_c (g)	d_o^* (μm)	A_o'	n'
MS/NiAl/Indian	0.9955	8.96	0.11	1.883	311	70.28	330.6	1.89
MS/NiAl/Imported	0.9989	7.53	0.13	1.809	226	65.36	252.9	1.81
MS/NiAl/PDZ	0.9977	4.05	0.21	1.585	141	70.47	179.4	1.59
MS/NiAl/Zircon	0.9893	3.92	0.14	1.700	473	131.00	578.2	1.70
MS/NiAl/Zircon-20 wt% calcia	0.9995	6.44	0.198	1.704	327	85.00	379.5	1.69

r^2 is the linear correlation coefficient for linear fitting.

is a high amount of correlation between d and $P^{1/2}$. In most of the cases, the correlation coefficients are found to be near 0.99, and it suggests that the experimental results are in close agreement with Equation 4. Now from the slope of the linear curve, the true hardness, H_o, values are calculated and the results are shown in Table II. The Indian alumina is found to be slightly harder than its imported counterpart. The hardness of the PDZ and the zircon coatings fall in the same range. This is expected since both of these coatings have a similar chemistry and microstructure. The zircon-20 wt% CaO coating registers a higher hardness value owing to the chemical stabilisation of the harder cubic zirconia phase.

The true hardness, H_o, is independent of the indentation load and may be viewed upon as a parameter independent characteristics of the coatings. Table III shows the various values of the ratio b'/a' for the coatings at different indentation loads and the H/E values.

TABLE III Various hardness values and elastic modulus of top coats under varying loads

Top coats	Load (g)	KHN	b'/a'	H/E	E(GPa)
Al_2O_3 (Indian)	25	1074	0.121	0.0427	251
	50	1077	0.116	0.0542	199
	100	1105	0.117	.052	212
	200	1032	0.116	0.0547	188
	300	842	0.106	0.075	111.8
	500	991	0.114	0.0578	171.3
Al_2O_3 (Imported)	25	1135	0.123	0.038	295
	50	914	0.116	0.054	168
	100	973	0.112	0.0629	154
	200	846	0.119	0.048	176
	300	800	0.113	0.060	132
	500	837	0.115	0.055	152
PDZ	25	934	0.115	0.0556	167
	50	720	0.117	0.0505	142
	100	491	0.100	.088	55
	200	516	0.111	0.065	78.6
	300	498	0.112	0.0625	80.01
Zircon	25	875	0.106	0.075	116
	50	670	0.109	0.070	95.5
	100	721	0.115	.0559	154
	200	688	0.113	0.060	113.4
	300	559	0.116	0.0547	102
	500	428	0.111	0.0648	66
Zircon 20 wt% CaO	25	1236	0.117	0.0511	234
	50	1005	0.119	0.0465	261
	100	968	0.115	0.0552	175
	200	881	0.121	0.0428	223
	300	758	0.118	0.0495	190
	500	744	0.124	0.0354	135

Substrate: Mild steel, Bond coat: NiAl.

It is observed that the b'/a' ratio varies with the indentation load. This is probably owing to the difference in elastic recovery at different indentation loads. For each indentation load, the H/E ratio is calculated according to the Equation 6. Using the corresponding hardness value at the same indentation load, the E value is evaluated. The E values of the coatings are found to be about one third of the bulk materials. This is especially true for the two alumina specimens. This reduction in E value is not only related with the amount of porosity but also with the morphology of the pores. It is postulated that the structure of boundaries between the splats have a considerable effect on the lowering of E values [17, 18].

3.3. Application of the Meyer's law, the Hays Kendall approach and the proportional specimen resistance model

Meyer's law correlates the indentation size diagonal, d, to the indentation load, P, in the following manner:

$$P = Ad^n \tag{7}$$

where the indices, A and n can be calculated, using the values of P and d obtained from the experiments [19]. Assuming the influence of ISE to be negligible, the parameter n assumes a constant value of 2 and under this circumstance the above equation reduces to the following expression, which is known as the Kick's law.

$$P = kd^2 \text{ [20].} \tag{8}$$

However, the experimentally obtained value of n is found to lie between 1 and 2, and it can be attributed to the presence of ISE. The values of A and n can be found out for each of the samples from the intercept and slope of a plot of $\ln(d)$ vs. $\ln(P)$. These values are listed in Table II.

It is to be observed that for all the samples the n value is found to be less than 2 which again indicates that there does exist an Indentation Size Effect for all the tested specimens. The calculated values of n show that the effect of the ISE for the two-alumina samples (Indian and imported) are similar. For the case of the zircon-20 wt% calcia and the zircon coatings, the ISE pattern according to Meyer's index are similar. However, PDZ,

though having essentially same composition as that of zircon or zircon-20 wt% calcia, shows a widely different value. Hence, it seems that, though Meyer's law throws some light on the ISE, it is not entirely satisfactory. It is not a very sensitive tool for explaining the phenomenon.

The Equation 7 represents a peculiar dimensional dilemma. The units of A according to dimensional analysis is $F[L]^{-n}$ whereas, the parameter n is dimensionless. Thus, it is observed that the dimension of the coefficient A depends on the value of n. Hence, for each specific n value the dimension of A is different [20]. So the plot of A vs. n is difficult to conceive from the dimensional point of view. Thus, the need for a normalised form of the Meyer's law arises. Meyer's law can be normalized as

$$P = A_o(d/d_o)^n \tag{9}$$

where, A_o now has the unit of force and n is the dimensionless parameter.

The parameter d_o must then have the dimension of length. The d_o term may be physically related to the true hardness H_o through Equation 1. Thus, the value of d_o has to be calculated from the value of H_o. However, it should be noted that the characteristic indentation size that corresponds to the "true" hardness does not really exist until the indentation size effect or load effect is diminished during indentation process. So it is important to find out this characteristic indentation size d_o^*. The expression for this 'non-load' effect criterion is of the form $dH/dP = 0$ with which a constant load-independent hardness H_o as well as a critical test load P_c and a corresponding d_o^* value can be associated. Since the microhardness is a function of the indentation test load, the general expression of this function can be obtained by differentiating Equation 1.

$$dH/dP = 14229\{d - 2P(\partial d/\partial P)\}/d^3 \tag{10}$$

$$\partial d/\partial P = (nAd^{n-1})^{-1} \quad \text{[from Equation 7]} \tag{11}$$

Substitution of the value of $\partial d/\partial P$ in Equation 10 yields

$$dH/dP = 14229\{d - 2P(nAd^{n-1})^{-1}\}/d^3 \tag{12}$$

Applying the criterion of load independent hardness, Equation 12 reduces to

$$P_c = (n/2A)(d_o^*)^n \tag{13}$$

where P_c is the critical indentation load [21]. In this final form of the equation, we have put the A and n values as obtained from the analysis of Meyer's law. Then using the hardness equation, $H_o = 14229\,P_c/d_o^{*2}$ and replacing P_c using Equation 13, the characteristic indentation sizes of the various coatings are obtained and then P_c can be computed putting in the values of d_o^* in Equation 13. The values of d_o^* and P_c for the various samples are listed in Table II.

This d_o^* value can now be utilised to develop a revised Normalized Meyer's law

$$P = A'_o(d/d_o^*)^{n'}. \tag{14}$$

A plot of $\log P$ vs $\log(d/d_o^*)$ is made for each of the coatings. A high correlation of around 0.99 exist for the plot of $\log P$ and $\log(d/d_o^*)$ for all the samples. These plots yields the values of A'_o from the intercept of the best fitted line and the n' value from the slope of the line. The A'_o and the n' values obtained are shown in the Table II.

The calculated A'_o values lie within the range of 179.4 grams to 578.2 grams. The indentation size or load effect can now be addressed utilizing the revised normalized Meyer's Law coefficient, i.e., the A'_o value. The following relation among A'_o, A and d_o^* can be derived

$$A'_o = A(d_o^*)^n. \tag{15}$$

A comparison between Equations 13 and 15 gives $A'_o = 2P_c/n$. Therefore, the normalized Meyer's law (Equation 14) assumes the following form.

$$P = 2P_c/n(d/d_o^{*^*})^n \tag{16}$$

It is now clear that the indentation size effect can be effectively related with the two physical parameters, P_c and d_o^*, which can be derived from experimental data. The advantage of using normalized Meyer's Law is that the parameter A with its complicated dimensional nature gets eliminated and in its place a critical load factor, P_c come into play. Again this P_c is related to the load independent hardness and to the characteristic indentation size, d_o^*. The n' values obtained from revised normalized Meyer's law is almost indentical to the n values obtained from the Equation 9, and hence it appears that the normalized Meyer's law also does not explain the ISE completely. A list containing both n and n' values for all the coated samples are included in Table II.

An alternative approach to the explanation of the ISE phenomenon has been put forward by Hays and Kendall [22]. It has been proposed that the basis of the ISE is the existence of a minimum level of the indentation test load, W_i, below which permanent deformation or flow does not initiate, but only elastic deformation occurs. The following equation for the analysis of microhardness data has also been formulated

$$P = W_i + kd^2 \text{ [22]} \tag{17}$$

where k is a constant.

At lower loads the fraction of the load, which brings about deformation, i.e., $(P - W)$ is quite low, and the corresponding indentation size is very small. This in turn results in an abnormally high hardness value. This effect gradually diminishes with the increase in load. A linear regression analysis of P vs d^2 has been carried out and from the intercepts of the best fitted lines, the W_i for the various samples are obtained. They are shown in the Table IV.

TABLE IV Values of W_i, n_w, a_1, a_2, for various coatings

Sample type	W_i (g)	n_w	a_1	a_2
MS/NiAl/Indian	6.72	2.05	0.370	0.0617
MS/NiAl/Imported	7.61	2.00	0.440	0.0522
MS/NiAl/PDZ	11.64	1.94	0.676	0.0267
MS/NiAl/Zircon	17.41	2.27	0.960	0.0255
MS/NiAl/Zircon-20 wt% CaO	20.29	2.52	0.822	0.0440

These W_i values seem to be quite large; especially the values for zircon and zircon-20 wt% calcia appear to be quite high. It seems that there is an overestimation of the Wi value when applying the Hays Kendall type of analysis to the Knoop indentation data of the plasma sprayed ceramic coating. This approach implies that the test load/indentation power law must always have an exponent of 2 and the load, P, is replaced by P_{eff}, which equals $(P - W_i)$. Here it is necessary to find out whether the selection of the value of the exponent is appropriate or not. This can be done by further examination of the Equation 17 expressed in the logarithmic form. The exponent, now redefined as n_w is taken as a variable instead of the constant equal to 2. Rewriting of Equation 16 in the logarithmic form yields

$$\log(P - W_i) = \log k + n_w \log d \tag{18}$$

If it is assumed that the indentation load/size effect is a result of the sample resistance, W_i, to the material flow, then the linear regression analysis of Equation 18, using the previously determined W_i values should yield the n_w value as 2 for all the experimentally obtained microhardness results. Table IV summarizes the values of n_w obtained for various samples using this technique of linear regression.

The n_w values as observed, are always nearly equal to 2 except for the zircon-20 wt% calcia sample where it shows a considerable variation from the ideal value of 2. Considering the fact that for most of the samples, the n_w is close to 2, it may be inferred that the Hays Kendall approach does have some merit for the present analysis. However, the unrealistically large W_i values indicate that this approach has failed to explain the ISE phenomenon fully.

The Proportional Specimen Resistance model as developed by Li and Bradt [12] also has been applied to the ceramic coated samples. This approach suggests a Newtonian like proportional specimen resistance (PSR) that is directly proportional to the magnitude of the indentation size. The PSR model in its mathematical form is shown below

$$P = a_1 d + a_2 d^2. \tag{19}$$

$$\text{or} \quad P/d = a_1 + a_2 d \tag{19A}$$

A linear regression analysis is carried out for P/d vs d plots and from the intercepts and slopes of the lines the a_1 and a_2 values are calculated. These are listed in Table IV.

In this model the physical meanings of the two PSR parameters, i.e., a_1 and a_2 have been very effectively addressed. It is proposed that the a_1 value consists of two complementary effects: (i) the elastic resistance of the test specimen and (ii) the indenter facet/test specimen interfacial friction. The values of the a_1 for both the alumina (Indian and imported) samples are almost similar. The little difference may be accounted for the change in the interfacial friction arising between the indenter and the test spcimen owing to the presence of some different phases in the two specimens as found from the X-ray diffraction study of the two samples (Table I).

The a_1 value of the PDZ coating is higher probably because of a high elastic resistance of this sample. The increase in the elastic resistance may be accounted for by the presence of a glassy silica phase in the coating. For zircon and zircon-20 wt% CaO, the a_1 values are even higher. For the zircon-20 wt% CaO coating the a_1 value is the highest. This can be attributed to the presence of the hard cubic zirconia phase, which gets stabilised owing to the addition of calcia. This hard phase causes an increase in the friction between the indenter/test specimen facet, thereby increasing the a_1 value.

It has been suggested [20] that the a_2 value is related to the true hardness of the specimens. It is observed that the a_2 value is highest for the Indian alumina coating which does have the highest true hardness among all the top coats. The a_2 value for the imported coating is slightly lower than the one obtained for the Indian coating. This is also consistent since the true hardness value for this imported coating is less than that for the Indian coating. The a_2 values for the PDZ and the zircon coatings are almost same which is in agreement with the fact that there is little difference in the true hardness of the PDZ and the zircon coatings. However, for the zircon-20 wt% calcia coatings, the a_2 value differs widely from the a_2 values of the PDZ and the zircon coatings. This is expected since the true hardness value of the zircon-20 wt% calcia coating is high. The higher true hardness of this coating again can be attributed to the presence of the hard cubic phase, which has been stabilized by the addition of the excess amount of calcia. The a_2 values of the different coatings can thus be correlated to the true hardness of the samples.

4. Conclusions

This investigation addresses the indentation responses of a few plasma sprayed ceramic coatings. It is observed that the Vickers hardness values of the plasma sprayed ceramic coatings are always consistently lower than the corresponding hardness values of the sintered ceramics. This trend of hardness values can be attributed to the unique microstructure of the coatings. The Indian alumina coating exhibits a distinct Indentation Size Effect (ISE) phenomenon whereas the PDZ and zircon coatings show a Reverse Indentation Size Effect (RISE) phenomenon. Based on the above observations, it can be inferred that brittle ceramic coatings can exhibit both types of indentation phenomenon (ISE and RISE) based on the composition of the coatings. It is alos observed that the hardness values of these coatings vary considerably with indentation load. Calculation of

K_{IC} and interpretation of wear behaviour based on hardness concept requires a single hardness value. The concept of 'true hardness' independent of the load is thus helpful.

In the present study, true hardness values for all the plasma sprayed ceramic coatings on mild steel substrates are determined. E values of the coatings are obtained using the elastic response in the elastic-plastic field during Knoop indentation tests. The method is much less time consuming and can be used as an attractive tool by the quality control monitoring unit for the plasma sprayed ceramic coatings. In addition, the elastic anisotropy of these coatings can be deciphered using this simple technique. The E values of the coatings are found to be lower than those of sintered materials owing to the porosity, the pore morphology, the anisotropic character of the microstructure, and the interlamellar structure of the coatings.

Meyer's Law, Normalized Meyer's Law, Hays Kendall Approach, and Proportional Specimen Resistance models are applied to the Knoop indentation data obtained for the various plasma sprayed ceramic coated samples. It is apparent that Meyer's Law and Hays Kendall approach are not totally successful in explaining the ISE exhibited by the different ceramic coatings. The Proportional Specimen Resistance model on the other hand can explain the ISE more effectively. The significance of the a_1 and the a_2 values is established and the relationship between a_2 and the true hardness can be directly determined. It appears that the PSR model is valid for interpretation of indentation behaviour of the brittle ceramic coatings.

Acknowledgement

The authors wish to thank Dr. Sarama Bhattacharya of the Regional Research Laboratory, Bhubaneswar, India for kindly providing them with plasma dissociated zircon and zircon sand. Financial assistance received from the Council of Scientific and Industrial Research, New Delhi, India to carry out a part of this research is gratefully acknowledged.

References

1. K. NIIHARA, R. MORENA and D. P. H. HASSELMAN, *J. of Mater. Sci. Lett.* **1** (1982) 13.
2. ZHUANG LI, ASHIS GHOSH, ALBERT S. KOBAYASHI and RICHARD C. BRADT, *J. Amer. Ceram. Soc.* **72** (1989) 904.
3. R. MCPHERSON and P. CHEANG, "High Performance Ceramic Films and Coatings" (Elsevier, New York, 1991) p. 277.
4. H. LAUSCHMANN, M. MORAVCOVA, K. NEUFUSS and P. CHRASKA, "Thermal Spray Industrial Applications" (ASM International, Materials Park, OH, 1994) p. 669.
5. D. B. MARSHALL, TATSUO NOMA and A. G. EVANS, *Comm. of the Amer. Ceram. Soc.* **65** (1982) 175.
6. G. R. ANSTIS, P. CHANTIKUL, B. R. LAWN and D. B. MARSHALL, *J. Amer. Ceram. Soc.* **64** (1981) 533.
7. S. K. SHETTY and I. G. WRIGHT, *J. of Mater. Sci. Lett.* **5** (1986) 365.
8. P. M. SARGENT and T. F. PAGE, *Proc. Br. Ceram. Soc.* **26** (1978) 209.
9. S. P. TIMOSHENKO and J. N. GOODIER, "Theory of Elasticity" (McGraw Hill, New York, USA, 1970) p. 191.
10. SANG-HA LEIGH, CHUNG-KWEI LIN and CHRISTOPHER C. BERNDT, *J. Amer. Ceram. Soc.* **80** (1997) 2093.
11. P. P. BANDHYOPADHYAY, PhD thesis, IIT Kharagpur, India, 2000.
12. H. LI and R. C. BRADT, *J. Mater. Sci.* **28** (1993) 917.
13. H. LI, A. GHOSH, Y. H. HAN and R. C. BRADT, *J. Mater. Res.* **8** (1993) 1028.
14. P. FELTHAM and R. BANERJE, *J. Mater. Sci.* **27** (1992) 1626.
15. HONG LI and R. C. BRADT, *ibid.* **31** (1996) 1065.
16. Report No. T/SM/20/1/92, Regional Research Laboratory, CSIR, India.
17. R. MCPHERSON, *Surf. Coat. Tech.* **39/40** (1989) 173.
18. J. P. SINGH, M. SUTARIA and M. FERBER, *Ceramics Engg. and Science Proceedings*, **18** (1997) 191.
19. E. MEYER, *Phys. Z.* **9** (1908) 66.
20. HONG LI and R. C. BRADT, *Journal of Non-Crystalline Solids* **146** (1992) 197.
21. *Idem.*, *Mater. Sci. and Eng.* A **142** (1991) 51.
22. C. HAYS and E. G. KENDALL, *Metallurgica* **6** (1973) 275.

Received 11 July 2001
and accepted 13 December 2002